Reactive Uptake of Ozone by Aerosol-Associated Unsaturated Fatty Acids: Kinetics, Mechanism, and Products

Tamar Moise and Yinon Rudich*

Department of Environmental Sciences, Weizmann Institute, Rehovot 76100, Israel

Received: February 4, 2002; In Final Form: April 10, 2002

The heterogeneous reaction between ozone and oleic and linoleic acids, prevalent components of both marine and urban organic aerosol, were studied in a flow reactor using electron impact and chemical ionization mass spectrometry. Liquids and frozen liquids were used as proxies for atmospheric aerosol. The reactive uptake coefficients, γ, were determined to be $(8.3 \pm 0.2) \times 10^{-4}$ and $(1.2 \pm 0.2) \times 10^{-3}$ for liquid oleic and linoleic acid respectively and $(5.2 \pm 0.1) \times 10^{-5}$ and $(1.4 \pm 0.1) \times 10^{-4}$ for frozen oleic and linoleic acid, respectively. Although, the reacto-diffusive length is estimated to be rather small in the liquid experiments, <10 nm, a clear indication of the participation of subsurface layers in the uptake is observed. This is in contrast to uptake by the frozen acids where the reaction is limited to the surface. Aldehydes were identified as the major volatile reaction products: 1-nonanal was detected following reaction with oleic acid, 2-nonenal, 4-nonenal, and 1-hexanal were detected following reaction with linoleic acid. The aldehyde yield, defined as the amount of the volatile product released relative to the ozone consumed, is dictated by its solubility in the liquid and frozen liquid acids. Azelaic acid was identified as a liquid-phase reaction product following the reaction with oleic acid. The implications regarding the atmospheric aging of aerosols with a fatty acid component are discussed.

Introduction

The way that tropospheric aerosols modify regional and global climate, via direct and indirect radiative effects and also via their influence on the Earth's hydrological cycle, has been the focus of many recent studies[1−5] following the recognition that aerosols play a dominant role in climate determining processes.

Field measurements have shown aerosol-associated organic matter to be ubiquitous in the atmosphere[6−9] and often associated with inorganic aerosols,[10−13] cloud droplets[14,15] and cloud condensation nuclei.[16,17] The need to understand and quantify the way by which the organic component of aerosols affects the aerosols' properties has led to a present-day focus on observations and measurements of organic aerosols in field measurements[18−20] and on laboratory studies to understand their formation mechanisms[21−23] and chemical and physical properties.[24−26] Studies demonstrating the modification of the organic aerosols properties as they undergo heterogeneous reactions in the troposphere have established the importance not only of freshly formed aerosol particles, but also, and even more so, that of aged particles.[27−29]

Laboratory studies on the reactivity of tropospheric oxidants with various model systems for organic aerosols; organic liquids, interfacial liquids, coatings and monolayers, have contributed both kinetic and mechanistic information regarding the heterogeneous chemistry of atmospheric organic aerosols.[27,28,30−34] Single aerosol particle mass spectrometry, initially developed for in-situ characterization of size-resolved atmospheric particles mass and chemical composition,[18,35,36] has recently been implemented also for laboratory studies of heterogeneous reactions of liquid aerosols.[36−39] Specifically, Morris et al.,[37] and Smith et al.,[39] have recently studied in detail the interaction of ozone with laboratory-generated liquid oleic acid aerosols.

This study provides complementary information regarding the ozone-oleic acid interaction. We focus on the reaction of ozone with unsaturated organic fatty acids, a significant component of airborne organic aerosol matter,[14,40] using liquid and frozen liquid substrates as proxies for atmospheric organic aerosols. The use of the liquid and frozen phases enables to differentiate between the bulk and surface contributions to the measured reactivity of the organics toward ozone. This study yields the reactive uptake coefficient, γ, and monitors the volatile and some of the liquid-phase reaction products. We examine the reaction of ozone with an unsaturated acid, oleic ($C_{18}H_{34}O$), and an acid with two unsaturated bonds, linoleic ($C_{18}H_{32}O$), to determine the effect of multiple reactive sites on the reactive uptake probability and on the products.

Much of the fatty acid load in marine aerosols is of oceanic origin.[41] Unsaturated fatty acids are major lipid compounds in the marine micro-algae and are enriched in the microlayers of sea-surfaces.[42] They are injected into the atmosphere by a bubble bursting process driven by winds.[43] The long chain hydrophobic organics remain adsorbed on aqueous atmospheric aerosols via their polar functional group, to form a surfactant coating over the surface of the aerosol.[44,45] Specifically, long chain monocarboxylic acids ($C_{14}-C_{18}$) have been identified over the marine atmosphere[41,42] and acids of C_{12}, C_{14}, C_{16} and C_{18} have been shown to be the predominant lipids in Antarctic summer aerosols.[46] Smaller acids have been shown to predominate the acid content in rain droplets collected in urban regions.[47] The thermodynamic properties of short chain acids (C_1-C_4) predict a saturated surface coverage of these species over water droplets, and indicate that these organic molecules are partially solvated at the air−water interface.[48]

Oleic acid has also been shown to be a significant fraction of continental organic aerosol matter. In urban environments,

10.1021/jp025597e CCC: $22.00
Published on Web 06/12/2002

TABLE 1: Reactive Uptake Probability, γ, of Ozone by Liquid and Frozen Oleic and Linoleic Acid

		T (K)	γ liquid	T (K)	γ frozen
Oleic	$C_{18}H_{34}O_2$	286−291	$(8.3 \pm 0.2) \times 10^{-4}$	267−275	$(5.2 \pm 0.1) \times 10^{-5}$
Linoleic	$C_{18}H_{32}O_2$	274−265	$(1.2 \pm 0.2) \times 10^{-3}$	254−265	$(1.4 \pm 0.1) \times 10^{-4}$

The error is the standard deviation (1σ) of all γ values contributing to the average.

its main source is meat charbroiling and traffic emissions.[6,40,49] An additional contribution arises from the abrasion of particulate matter from leaf surfaces of urban plants.[50] In rural environments, its main source is biogenic emissions, both directly and via secondary aerosol formation.[49] Oleic acid has been used as a mass balance tracer for emission inventories by Schauer et al.[40] and in that study, it was assumed to be an inert species within the geographical dimensions monitored.

Experimental Section

The reactive uptake of ozone by oleic (*cis*-9-octadecenoic) and linoleic (*cis*,*cis*-9,12- octadecadienoic) acids (Fluka, ∼99.5%) in their liquid and frozen states was studied using a cylindrical rotating wall flow reactor coupled to a mass spectrometer.[31,34,51] The experimental system has been described in detail previously[31] and only specifics relevant to the current measurements are described here. The reactive uptake coefficient was determined from the first-order loss rate of gas-phase ozone,[52] detected as O_3^- following its chemical ionization by SF_6^-. Ozone was injected into the reactor through a moveable injector and interacted with the organic compounds coating the rotating reactor's inner walls. Ozone concentrations of approximately 10^{10} molecules cm^{-3} were used for the uptake measurements. Typical pressures and velocities in the reactor were 3−9 Torr and 50−200 cm sec^{-1} respectively. Helium was used as the carrier gas. Laminar flow was established in the flow tube <1 cm downstream from the gas inlet. The host reactor was temperature regulated and insulated from its surroundings by an outer vacuum jacket. The temperature was monitored using a thermocouple inserted via the moveable injector and it was verified that there was no temperature gradient along the reactor path length.

Volatile reaction products were monitored using electron impact mass spectroscopy and ozone concentrations of $\sim 10^{14}$ molecules cm^{-3}. Product concentrations were estimated by using calibrated flows of 1-butene and comparing peak intensities of shared fragments taking into consideration their respective relative yields.

Liquid reaction products were analyzed in their anionic states using ion chromatography (IC). A high performance liquid chromatography (HPLC) unit (Varian Prostar) was equipped with a Dionex AS 11 analytical column and a Dionex (ED50) Electrochemical Detector. The elution strength of the mobile phase is controlled using a gradient eluent with concentrations ranging from 0.4 mM NaOH to 22.5 mM NaOH. The liquid organics were dissolved in a 5 mM NaOH solution prior to injection.

Results

1. Reactive Uptake Coefficients. The reactive uptake coefficients of ozone, γ, were determined at a range of temperatures below and above the melting point of oleic and linoleic acid using ozone concentrations in the range of $8 \times 10^9 - 2 \times 10^{11}$ molecules cm^{-3}. The measured loss rates were corrected for gas-phase concentration gradients caused by the O_3 uptake, using the method developed by Brown.[53] The diffusion coefficient for O_3 in He was taken as 394 Torr cm^2 s^{-1} at 298 K using the empirical equation formulated by Fuller et al.,[31,54] The ozone loss rate was much smaller than the gas-phase diffusion-limited loss rate, and hence the diffusion corrections were less than 20% for the highest measured uptakes. There are no significant differences in the γ values for each acid within the temperature range measured for a specific phase (liquid or solid) and the average γ for each phase is shown in Table 1. A distinct decrease in the reactive uptake coefficient (by at least an order of magnitude) is observed upon freezing of both organic acids. The values are plotted together with previously measured γ for the ozone reaction with aliphatic alkene chains[31] in Figure 1. The plot denotes a similar sharp decrease in γ upon lowering the reactor temperature to below the hexadecene freezing point. In addition, γ values are shown for liquid octene and a self-assembled octene monolayer which is a unique proxy for a surface limited reaction.[27,28,31,55]

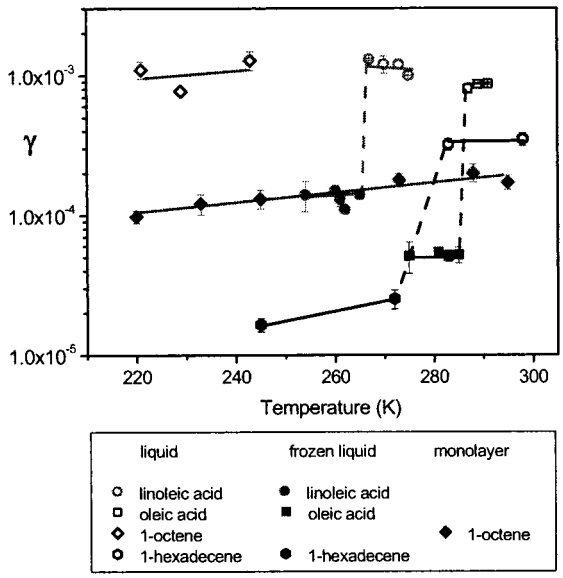

Figure 1. Reactive uptake coefficients of ozone for liquids, frozen liquids and monolayers of aliphatic alkenes and unsaturated acids. The γ values for reaction with the aliphatic alkenes are taken from *Moise and Rudich.*[31] The error is either the standard deviation (1σ) of all runs, or for temperatures at which the number of experiments was limited, an estimated error of 15%.

2. Volatile Products. *Product Identification.* Volatile products from the ozone and fatty acid reactions were monitored using electron impact mass spectrometry with 70 eV electrons and at ozone concentrations in the range of $5 \times 10^{13} - 5 \times 10^{14}$ molecules cm^{-3}. In these experiments, the acids were placed in an elongated "boat shaped" glass container which was inserted into the flow reactor.[56] As for the kinetic experiments at lower concentrations, the ozone loss rates did not vary within the range of concentrations used, and for temperatures ranging between just above the freezing point to ∼25° above it.

The electron impact mass spectrum following ozone reaction with oleic acid shows the volatile reaction products (Figure 2). The mass peak assignment and the relative intensities within closely spaced masses are uniquely assigned to 1-nonanal. The parent peak masses at $m/e = 141$ and 142 are also identified. The relative intensities between distant masses differ from the

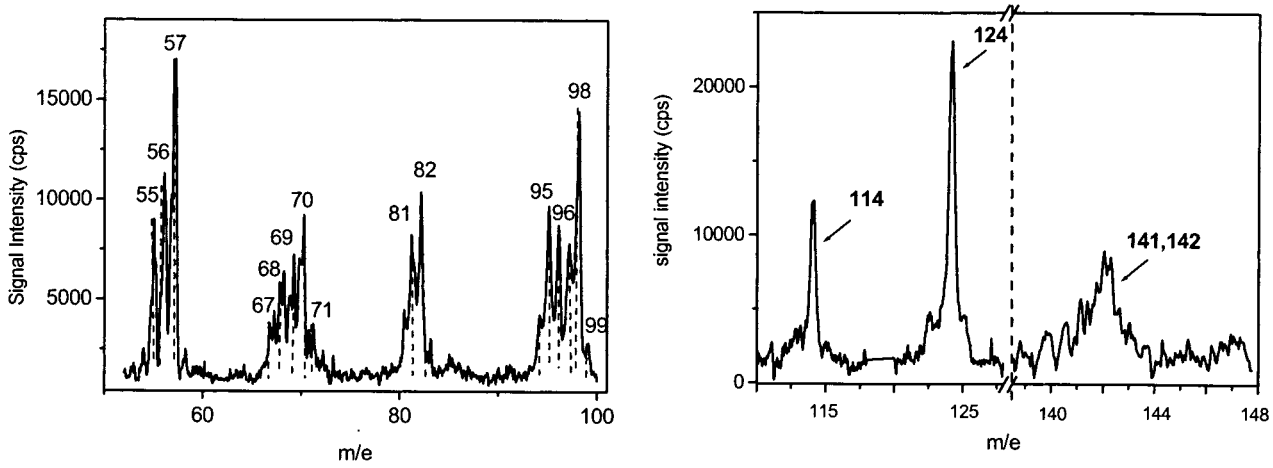

Figure 2. Mass spectrum of the volatiles released from the ozone and oleic acid reaction shows the only detected product to be 1-nonanal.

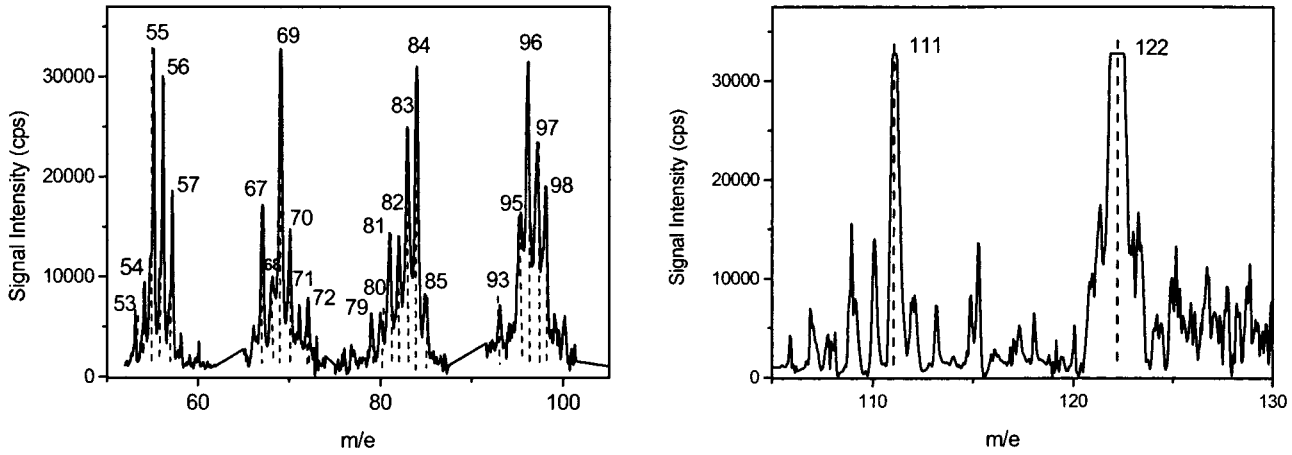

Figure 3. Mass spectrum of the volatiles released from the ozone and linoleic acid reaction. The products are identified as 2-nonenal, 4-nonenal and 1-hexanal.

National Institute of Standards and Technology (NIST) standard library spectrum due to the use of the quadrupole mass spectrometer in a mass dependent ion-transmission mode that discriminates against the high masses.

The mass spectrum observed following the reaction of ozone with linoleic acid is more complex and depicts a number of volatile products (Figure 3). The spectrum is compatible with the presence of 2-nonenal and 4-nonenal, identified explicitly from the higher mass peaks ($m/e = 111$ and 122) and compatible with the relative intensities of many of the lower mass peaks. The rate at which the peaks intensities vary when the temperature of the reactor is changed assembles them into two distinct groups (Figure 4). The peaks at $m/e = 56$, 57, 72, and 82 all display a similar slope, which differs from that of the other major peaks associated with the nonenal products. These four masses are the major peaks of the 1-hexanal mass spectrum (at $m/e >$ 50). The peak intensities at $m/e = 69$ and 95 are still larger than expected if 1-hexanal and 2- and 4-nonenal are the only products, suggesting there may be an additional obscured volatile product.

Volatile Products Release to the Gas-Phase. The intensity of the reaction products signal decreased when the liquid organics were cooled. A steeper decrease was observed immediately at the phase change (Figure 5). For linoleic acid, the signal decrease with temperature of 1-hexanal was gentler than that of nonenal (Figure 4).

In contrast to its absolute concentration, the rate of product release from the liquid reaction remains constant within the same

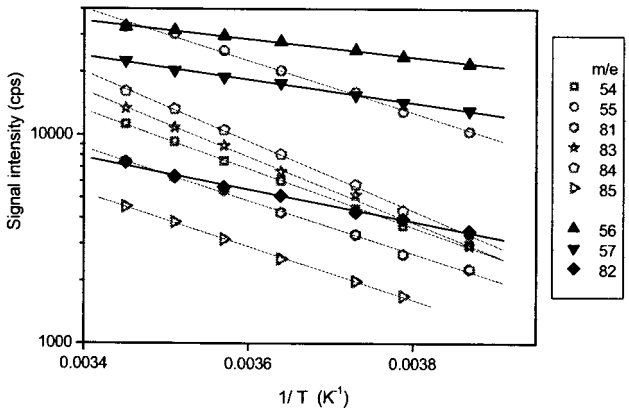

Figure 4. Changes in the signal intensities of various peaks of the reaction products of linoleic acid as the reactor is cooled. Two main slopes are observed, grouping the peaks into 2 assemblages. The peaks designated by black symbols are assigned to the 2-nonenal and 4-nonenal products. The peaks designated by gray symbols are assigned to the 1-hexanal product. (The peak at $m/e = 72$ was shown in different runs to have a slope as that of the 1-hexanal products).

temperature range (Figure 6). The equation describing the growth of the product in the gas-phase is

$$P = A_0 (1 - \exp^{(-kt)}) \quad (1)$$

where P is the product intensity, A_o is the asymptotic product intensity, k ($\sec^{-1}$) is the growth rate constant, and t (sec) is

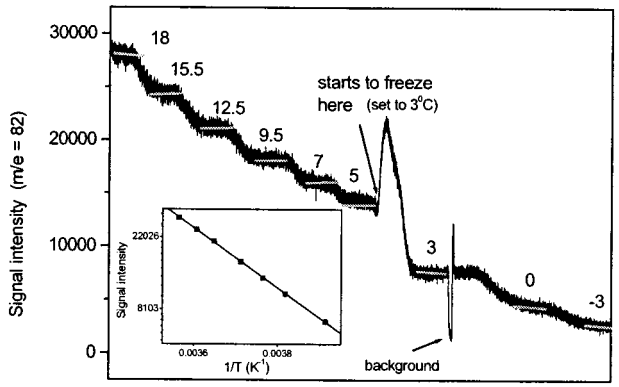

Figure 5. Decrease in the concentration of the reaction product ($m/e = 82$) on cooling of the reactor while reacting ozone with oleic acid. The injector is kept at a fixed position. The numbers are the temperature in Celsius for each time span. As the liquid starts to freeze, the product yield first increases and subsequently decreases once the liquid is entirely frozen. At this stage a sharp decrease in product formation is observed. The inset shows the decrease to be exponential (the *Y* axis is a ln scale). The background is the signal measured when the ozone flow over the organic liquid is stopped.

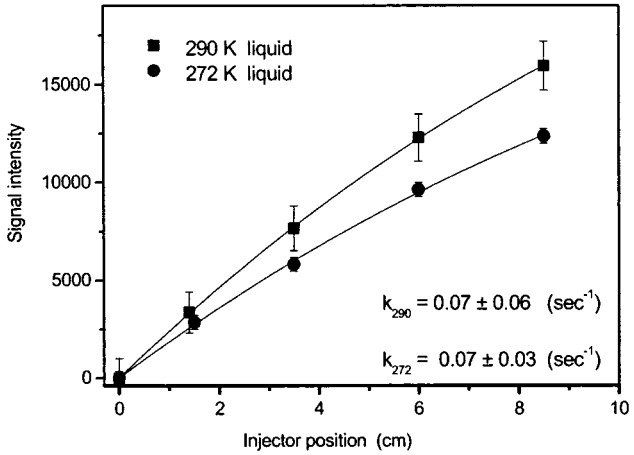

Figure 6. Growth of the aldehyde products following reaction of ozone with linoleic acid. The *x* axis is the position of the moveable injector and defines the interaction time. The yield of the aldehyde product decreases as the liquid temperature decreases. The formation *rate* however, remains constant ($T = 290$ and 272 K). The growth rate constant, k, is obtained from the fit to eq 1.

the reaction time. For reaction with linoleic acid the growth was monitored for ion fragments associated with the different products ($m/e = 56$, 69, and 84). Within the accuracy of our measurements the rate of product release, which we define as the growth rate and is expressed by the constant k, was identical for all peaks.

Product Yield. The aldehyde product yield is defined as the ratio between the aldehyde concentration released to the gas-phase and the ozone concentration reacted. The yield was estimated by plotting the ozone loss vs the products growth (Figure 7). The products gas-phase concentration was estimated by calibrating the mass peak intensities at $m/e = 56$ with those of known butene flows, taking into consideration the respective relative yields of 1-butene and 1-nonanal at this mass. For liquid oleic and linoleic acid, the yield decreased as the reactor temperature is decreased. For example, the 1-nonanal yield following reaction with oleic acid at a temperature of 296 K was 28%, whereas at 279 K, but otherwise identical conditions, the yield decreased to 10%. When further decreasing the temperature and freezing the liquid, the reaction yield increased again to as much as 40%. The absolute amount of aldehydes

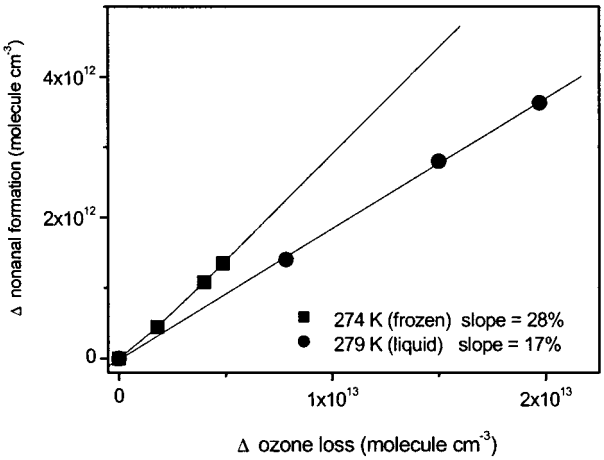

Figure 7. Slope of the ozone loss plotted vs the 1-nonanal released for the reaction of ozone and oleic acid. The slope yields the detected nonanal yield. Each point is for a different injector position, i.e different reaction times.

released from the frozen liquid was lower than that released from the liquid reaction. However, as the uptake of ozone is much lower for the surface reaction, the aldehyde yield per ozone reacted was greatly enhanced. This behavior was observed for a large number of experiments though quantifying the yield was difficult, leading to large errors.

The initial increase in product signal observed as the liquid begins to freeze (Figure 5) is attributed to the higher yield from uptake by frozen organics. The signal increase is observed only when a small fraction of the liquid is frozen over. However, as the liquid becomes completely frozen, the absolute amount of 1-nonanal product diminishes and despite the relatively high reaction yield, the total amount of released product remains smaller than that released from the liquid reaction. Alternatively, it is also possible that the product burst is due to physical expulsion of the aldehyde when the carboxylic acid freezes. If this is the case, not all the solvated aldehyde manages to escape prior to complete freezing. When a frozen oleic acid volume, previously exposed to ozone as it was cooled, was allowed to thaw with no further exposure to ozone, the release of previously solvated 1-nonanal was explicitly observed. As the frozen liquid started to melt, a surge of 1-nonanal was released as the interfacial "barrier" was disrupted and the pathway to the gas-phase became unrestricted.

The relative peak intensities were used to estimate the fraction of nonenal and 1-hexanal products. The ratio of nonenal to 1-hexanal decreased as the temperature decreased. For example, at $T = 285$ K nonenal:hexanal = 0.55:0.45, at $T = 284$ K nonenal:hexanal = 0.45:0.55 and at $T = 274$ K nonenal:hexanal = 0.30:0.70. The relative yield between 4-nonenal to 2-nonenal is similar at all temperatures, ~0.6:0.4, respectively.

3: Liquid-Phase Products. Polar products in both oleic and linoleic acids were analyzed using ion chromatography (IC). In these experiments, the ozone flow entered the reactor through a bubbler in which 1 cm^3 of the organic acids were placed. The liquid was continuously stirred to ensure ozone reaction with the entire liquid volume. The sample was then diluted in a 5 mM NaOH solution and injected into the IC. Use of a gradient eluent results in the elution of the stronger retained acids. Pure oleic and linoleic acids were also analyzed as reference spectra. Oleic acid showed 2 new dominant peaks following reaction. A broad peak at a retention time of 7.5 min tailing off only at 10 min, and a well resolved peak at 12.9 min. This second peak has a wide shoulder extending to ~15 min. Only the second

peak is identified beyond doubt and is assigned to the azelate ion, indicating the formation of azelaic acid ($C_9H_{16}O_4$) from the reaction. The first peak matches a hexanoic and heptanoic acid standard, which are difficult to resolve in our system. The shoulder tailing the azelate ion matches a nonanoic acid standard. Linoleic acid showed a similar constituent release at a retention time of between 7.5 and 10 min, indicating that the C_6-C_7 carbon products are common to both acids. However, only a very slight growth was observed at the peak of the azelate ion. For linoleic acid, additional unidentified peaks appeared at 16 and 18 min.

Discussion

1. Kinetics. The loss of ozone due to gas-phase reactions with the acids is negligible due to their low-vapor pressure[24] and all ozone loss is attributed to the reaction with the condensed phase. The decrease in the reactive uptake coefficient by at least an order of magnitude upon freezing of the organic acids (Table 1) is consistent with trends observed for measurements of ozone uptake by aliphatic alkenes (Figure 1) and for NO_3 uptake by aliphatic alkanes and a monocarboxylic acid.[30] The ozone uptake by the liquids was shown to have a significant contribution from reactions occurring in the bulk of the liquid, as much smaller γ values were observed when limiting the reaction to the surface via use of self-assembled monolayers.[31] The decrease in γ upon freezing of the liquid indicates that solubility, diffusion and reaction within the bulk of the liquid contribute substantially to the observed ozone and NO_3 uptake.[30,31]

For the case of uptake dominated by reaction in the bulk, assuming that $\gamma \ll \alpha$ (the mass accommodation coefficient), γ can be expressed according to the resistor model[57] as

$$\gamma = \frac{4RT}{\omega} H \sqrt{D_l k_l [\mathrm{X}]} \qquad (2)$$

where H is Henry's law coefficient (M atm^{-1}), D_l is the diffusion coefficient in the solute (cm^2 s^{-1}), k_l (M^{-1} sec^{-1}) is the second-order rate coefficient for reaction in the liquid phase, and [X] is the liquid-phase reactant activity. The square root factor arises from the solution of a bulk liquid reaction in which the gas-phase ozone flux across the interface is equated to the ozone flux within the liquid.[58] From eq 2, it follows that for uptake governed by bulk liquid reaction, doubling the reactant activity will result in an increase of γ by $\sqrt{2}$.

Assuming the activity of both acids to be similarly proportional to their concentration, and treating each unsaturated bond as contributing independently to the reactivity and having an identical rate constant, the ratio, R, between γ for the mono-unsaturated acid (oleic) and the di-unsaturated acid (linoleic) is expected to be

$$R = \sqrt{2 \times \frac{\rho_{\mathrm{linoleic}} \times \mathrm{MW}_{\mathrm{oleic}}}{\rho_{\mathrm{oleic}} \times \mathrm{MW}_{\mathrm{linoleic}}}} = 1.43 \qquad (3)$$

where ρ is the density (g cm^{-3}) and MW is the molecular weight (g mol^{-1}). The formulation of this term for R also assumes similar values of H and D_l for ozone in the two compounds. The actual measured ratio is 1.45 ± 0.19 suggesting that the reactant activity is directly related to the concentration of unsaturated bonds, supporting the conclusion that the uptake has a dominant contribution from reaction in the bulk.

For a surface reaction, represented by the frozen liquid, we would expect the reactivity to be directly proportional to the reactive site concentration at the surface and hence the ratio of γ of the frozen linoleic to the frozen oleic to be 2. The measured ratio between the γ values of the two frozen liquids is 2.6 ± 0.4. Possibly, differences in the surface concentration resulting from structural differences between oleic and linoleic acids, leading to a relatively higher availability of exposed unsaturated bonds for linoleic acid, are the cause.

A recent kinetic study of the ozone reaction with liquid oleic acid aerosols (200−600 nm diameter) by Morris et al.,[37] using ozone concentrations of about 2×10^{14} molecule cm^3, yields $\gamma = (1.6 \pm 0.2) \times 10^{-3}$ and compares well with our measurement for uptake in the liquid phase. Smith et al.,[39] observe a size dependent γ for the ozone reaction with oleic acid aerosols (1−5000 nm) which they attribute to diffusion limitation of the oleic acid to the surface. In our experiments, the rotation and mixing of the liquid would diminish any concentration gradient of the reacting acid from the depleted surface layers to the bulk of the liquid, and the uptake would not be affected by diffusion limitations. The γ value that is determined by *Smith* et al.,[39] for a nondiffusion-limited particle, i.e., an extrapolation of γ to zero particle diameter, is $\gamma = 5 \times 10^{-3}$, larger than γ measured in our experiments for nondiffusion limited uptake. Ozone uptake by canola oil, a mixture of mostly oleic, linoleic and linolenic acids, was also measured using flow tube experiments by deGouw and Lovejoy,[34] yielding a γ value of $\sim 7 \times 10^{-4}$ for the liquid and $\sim 2 \times 10^{-5}$ for the frozen liquid. In general, these values are in agreement with our measurements. It is not possible to assess the slight differences between these values and our own due to the mixture of the unsaturated fatty acids in the canola oil which for typical canola oils constitute ~90% of the total fatty acid content.

The measured reactive uptake coefficients are greater than those measured for long-chain terminal alkenes in our previous study.[31] To validate our experimental system, the uptake measurements were repeated for hexadecene. The γ values of the recent and previous experiments fall within the overall ± 25% error we associate with the measurements. The main factor contributing to this change are errors associated with determining the exact flow resulting from the fit of the rotating flow reactor within the main cylindrical reactor. The reaction of ozone with an unsaturated compound is an electrophilic addition,[59] and the presence of an electronegative substitute such as COOH is expected to lower the rate coefficient for reaction of the acid compared with the alkene.[59] However, the effect of the COOH group is hardly perceptible if the location of the polar group is at a distance greater than 3−4 carbons from the unsaturated bond as for the acids in our study.[59] The higher reactivity of the oleic and linoleic acids is probably due to the presence of substituted double bonds rather than the terminal unsaturated bonds of the long-chain aliphatic alkenes, in analogy to the gas-phase reactions.[59]

2. Products. Ozone loss is governed by reaction in the condensed phase and not from gas-phase reactions with the equilibrium acid vapor. It is necessary also to verify that the reaction products result only from the reaction with the condensed phase organics and are not the result of a minor pathway with gas-phase acids. This is validated by a number of arguments. (a) No products are observed when the injector is positioned downstream of the organic liquid, a configuration in which ozone cannot interact with the organic surface but is able to interact with gas-phase species, (b) taking the measured product formation rate and assuming that the products result from gas-phase reaction, the rate coefficient of ozone with the unsaturated acids would have to be between 5×10^{-14} to 5×10^{-13} cm^3 molecule^{-1} sec^{-1}, much larger than the estimated

gas-phase rate coefficient (approximately 1×10^{-17} cm^3 molec^{-1} sec^{-1} for unsaturated terminal and branched substituted alkenes[60,61]) c) the vapor pressure of linoleic acid close to the melting point is extremely low, $\sim 1 \times 10^{-9}$ Torr.[24] For conditions of ~9 Torr, total pressure and a flow of ~300 scc/min, this is equivalent to a gas-phase concentration of 3×10^7 molec cm^{-3}, much lower than the concentrations of the reaction products we detect and d) the reaction yield (discussed in the coming paragraph) is of a magnitude that shows this pathway to be a major pathway for the ozone loss which is dominated by reaction in the bulk.

Temperature Dependence of the Product's Yield. In contrast to ozone loss, which does not show a temperature dependence for either the liquid or frozen liquid, the product formation shows an exponential temperature dependence (Figure 5 inset). For ozone uptake, it would seem that the effect of the temperature dependencies of D_l and k_l are canceled by the contrasting temperature dependence of H. For the formation and release of the volatile product, the temperature dependence of the same three parameters could lead to a decrease in the observed signal due to (a) a decrease in the reaction rate coefficient, in analogy to the gas-phase, (b) a decrease in the branching ratio for the pathway leading to the aldehyde formation, (c) slower diffusion in the liquid phase, or (d) an increase in the aldehyde solubility and subsequently, less volatile release.

Diffusion out of the liquid matrix may be slowed on cooling, however, D_l is proportional to $T^{3/2}$ whereas the observed decrease is exponential. The exponential trend is compatible with the exponential trend for vapor pressure changes described by the Clausius−Clapeyron expression. In addition, the smaller decrease of the 1-hexanal product compared to the simultaneous decrease of the nonenal product (Figure 4) is compatible with the lower vapor pressure temperature dependence expected for smaller molecules. The temperature dependence of the nonanal (~nonenal) and hexanal vapor pressure over the pure substance can be estimated by the method of Makar.[62] This method yields slopes of 7670 (K^{-1}) and 5750 (K^{-1}) respectively when the natural logarithm of the vapor pressure is plotted against $1/T$. These are larger values than the slopes we measure of the signal intensity plotted against $1/T$. Repeated measurements of the 1-nonanal and nonenal slopes (monitoring various mass peaks) yield an average slope of 4000 ± 400 (K^{-1}) (Figure 5 inset). The 1-hexanal slope was measured less rigorously and gives a slope of ~1350 (K^{-1}). The estimated slopes will differ from the measured slopes as they express the vapor pressure over the pure parent liquid whereas the measured volatiles are dependent on the aldehydes solubility in the oleic acid.

We note then, that the estimates of the 1-hexanal and 2- and 4-nonenal yields reflect the solubility of the product rather than its actual reaction yield.

Possible Reaction Mechanism. Reaction Pathways: The mechanism of ozone reaction in the gas and liquid phases is via the insertion of ozone to the unsaturated bond to form a primary ozonide. The primary ozonide subsequently decomposes via the cleavage of one of the two O−O bonds and the C−C bond, whereas the stronger C−O bond remains intact to form a Criegee intermediate (biradical) and an aldehyde or ketone.[63,64] In solvents and in solids, the excess energy in the Criegee intermediate can be redistributed and solvent cage effects increase the probability that the Criegee intermediate will recombine with the carbonyl compound to form a stable secondary ozonide as the main reaction product.[63,64] In the gas-phase, the two fragments separate rapidly and the Criegee biradical, which contains excess energy, can stabilize or decompose in a number of channels leading to different products such as RCO, RCOOH, CO_2, CO, H_2O, and OH.[8]

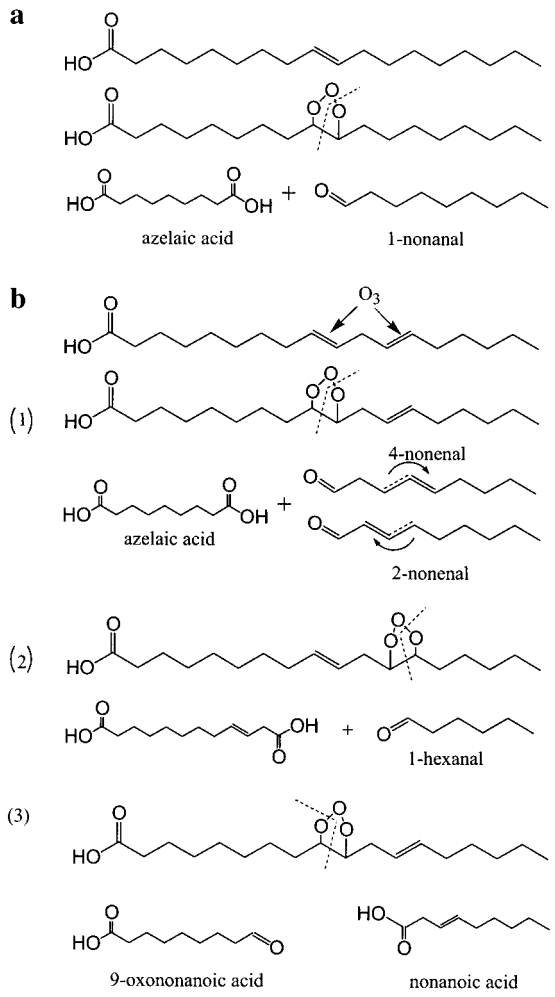

Figure 8. Reaction scheme for formation of volatile and liquid-phase products. The dashed line marks the place of scission of the O−O bond of the primary ozonide. (a) Formation of 1-nonanal and azelaic acid from the ozone reaction with oleic acid. 1-nonanal is partially released to the gas-phase while azelaic acid remains in the bulk liquid. (b) formation of (1) 2-nonenal and 4-nonenal, (2) 1-hexanal, and (3) nonanoic acid from the ozone reaction with linoleic acid.

The products observed in our experiments can form via the pathways shown in Figure 8. 1-nonanal and nonenal form via the cleavage of a primary ozonide formed at the C9 position (Figure 8a and 8b-1). For the linoleic acid (2 double bonds), the unreacted unsaturated bond at the now C3 position migrates to either the C2 and C4 position. The migration to the C2 position can be understood by recalling that the conjugation between the carbon−carbon double bond and the carbon−oxygen double bond adds stability to the molecule.[65] 1-hexanal can be produced from the primary ozonide formed at the C12 position (Figure 8b-2). Rearrangement of the Criegee biradical following stabilization can lead to the formation of dicarboxylic acids. Azelaic acid was observed following reaction with oleic acid and remains in the liquid phase due to its extremely low volatility (Figure 8a and 8b-1).

In addition, scission of the primary ozonide at the second peroxy bond will lead to additional products. The aldehyde will be associated with the acid fragment whereas the alkane fragment will yield the Criegee biradical (Figure 8b-c). Stabilized Criegee biradicals may rearrange to form a carboxylic acid or may react further with the acidic hydrogens and with the solvated aldehyde to form organic hydroperoxides and perox-

ides.[64,66] The product that tails the azelate ion at a retention time of ~14 min, following reaction with oleic acid, is compatible with a nonanoic acid standard representing the product from this second pathway. The product may well be nonanoic acid itself, expected to be formed from the intermediate Criegee biradical, or it may also be the original C_9 acid fragment with an aldehyde at the other end of the chain (Figure 8b-c). We are unable to differentiate between these groups of compounds. Similarly, the C_6 and C_7 assignment cannot be uniquely designated as the pure acid (as the standard) but also, may well be a bifunctional compound.

Reaction with Liquid Organics. The substantial yield of the aldehydes upon reaction with the acids indicates that for the pure organic liquids, the two fragments do not dominantly recombine to form the stable secondary ozonide, recognized as the main reaction product in solution.[59] This indicates less efficient "caging" and may be due to the reaction occurring mostly in the outer film of the bulk liquid. The depth to which reaction occurs can be estimated via estimation of the diffuso-reactive length, *l*, in the liquid, defined as[67]

$$l = \sqrt{\frac{D_l}{k_l^I}} \qquad (4)$$

where D_l(cm^2 sec^{-1}) is the diffusion coefficient of O_3 in the organic acids, and k_l^I(sec^{-1}) is the first-order loss rate of O_3 in the liquid. For oleic acid $k_l^{II} = 1 \times 10^6$ M^{-1} sec^{-1}.[59] D_l can be estimated from eq 2. Using H of 0.09 M atm^{-1}, the value for the much smaller acetic acid,[59] and our measured γ of 8.3×10^{-4}, D_l at 290 K is estimated as 1×10^{-6} cm^2 sec^{-1}. The diffuso-reactive length is then estimated to be ~6 nm. This indicates that the reaction occurs quite close to the surface.

Reaction with Frozen Organics. The observed increase in aldehyde yield for the surface reaction can result from two processes: (1) the aldehyde formation pathway is more significant than the same pathway for the bulk liquid reaction and (2) less efficient solubility. This is consistent with the reaction being limited to the surface where a less efficient caging is expected than for the liquid reaction. In addition, upon freezing, the diffusion of the reaction products to the interior of the liquid is greatly slowed, and the products are therefore released unidirectionally at the interface. The measured yield from the surface reaction of ~40% is on the same scale as the aldehyde yield observed in previous studies investigating ozone reactions on organic surfaces. Thomas et al.,[55] observed a 50 ± 10% yield of formaldehyde following the surface reaction between ozone and self-assembled monolayers composed of terminal aliphatic alkenes. Wadia et al.,[32] also observed nonanal formation following reaction between ozone and an unsaturated phospholipid (OPPC) at an air−water interface. Their observed yield is corrected for the partial solvation of the nonanal product in the aqueous phase and the total reaction yield is given as 54 ± 11%.

Atmospheric Implications. We observe that the ozone reaction with unsaturated fatty acids leads to the release of long-chain aldehydes. The tropospheric reaction of ozone with aerosol-associated unsaturated fatty acids can thus contribute to the oxidative capacity of the atmosphere via the aldehyde photolysis to alkyl radicals and HCO and subsequent production of HO_2.[8] The amount of aldehydes released will depend on the temperature of reaction, the solubility of the products in the aerosol phase and the ambient gas-phase concentrations.

Azelaic acid is one of the complementary refractory organics to the observed 1-nonanal and nonenal volatile products (Figure 8) and remains in the condensed phase due to its low volatility. Dicarboxylic acids are recognized as ubiquitous organic aerosol constituents.[49,68] Although diacids with higher carbon numbers are generally less abundant than the smaller acids, azelaic acid is shown to be a relatively common constituent in both urban and marine regions.[6,46] Analysis of aerosol measurements collected over the Mediterranean Sea showed that higher ratios of azelaic acid to unsaturated fatty acids were concurrent with higher ozone concentrations.[69] The maximal formation rate of the dicarboxylic acids can be estimated from the uptake values measured in our experiments, assuming that azelaic acid is formed in the same yield as 1-nonanal, i.e., at ~ 40%. A complete characterization of the soluble acids, hydroperoxides and peroxides that are formed is necessary for a rigorous estimate.

The dicarboxylic acids formed by the ozone-unsaturated fatty acid reactions are smaller and by far more polar than the parent fatty acid molecule and are thus more hygroscopic. Consequently, for aerosols with a high organic content, the product dicarboxylic acids can contribute to their cloud nucleation activity due to the enhanced water affinity.[25,70] In general, a mixture of organics will take up less water than that associated with each of the compounds in its pure form.[26] The relative hygroscopicity of atmospheric aerosol organics is diacids > monoacids > alcohols > carbonyls.[26]

Organic matter has been shown to contribute to the cloud nucleating portion of aerosol mass.[16,17] Specifically, the organic material that acts as cloud condensation nuclei (CCN) has been shown to be composed of water-soluble organic species.[17,71] The oxidation of volatile organic compounds and primary organic aerosols to form more polar and multi-functional compounds thus renders much of the tropospheric organic material to be water-soluble. In general, measurements of fine aerosol in background, rural and polluted regions show that over 70% of the organic compounds at all sites are of polar nature.[11] Aerosols collected in remote regions also show a predominance of polar organics.[72,73] The diacids and peroxides formed from the ozonolysis of the fatty acids may be examples of such organic CCN components.

As the dicarboxylic acids are highly water soluble, the ozone reaction with the fatty acids can modify the overall partitioning of organic matter between an aqueous particle, its surface and the gas-phase. The distribution of the organic material may be driven from a film-like coating of the amphiphilic parent fatty acids to solvation of the shorter polar chains within the bulk of the aqueous aerosol droplet. In aqueous droplets, additional low vapor pressure products such as organic hydroxy-hydroperoxides are expected to form and accumulate in the condensed-phase due to their extremely low volatility.[23]

The presence of a surficial organic coating can limit mass-transfer between the inner part of a particle and the ambient air. Ozonolysis, which breaks long molecules, will destroy such organic coatings and can enable mass-transfer across a previously "blocking" interface. Growth of the aerosol will also be promoted. The greater solubility of the dicarboxylic acids lowers the vapor pressure of the droplet due to the "Raoult Effect". This then lowers the critical super-saturation values[74] and increases the particles CCN potential. An opposing force to this process are the changes in surface tension that an aerosol coated by a fatty acid film may undergo. The shorter chain organic acids have a higher surface tension than the parent long chain acids[74] such that as the parent molecule reacts and the aerosol is processed there may be an increase in the surface tension which in turn would depress droplet growth.[15,74] This may be

offset however, by the composition transformation to polar groups which will further serve to reduce the surface tension, the overall result being a decrease in the critical supersaturation values for the processed aerosol.

These changes in composition and in the distribution of the organic components have many implications on the aerosols physical and chemical properties and need to be assessed and quantified.

Acknowledgment. We thank Alla Falkovitch for her help with the IC analyses. This work was partially funded by the US-Israel Binational Science Foundation (Project No. 1999134) and by the Minerva Science Foundation. Yinon Rudich is the incumbent of the William Z. and Eda Bess Novick career development chair.

References and Notes

(1) Ramanathan, V.; Crutzen, P. J.; Kiehl, J. T.; Rosenfeld, D. *Science* **2001**, *294*, 2119.
(2) Charlson, R. J.; Seinfeld, J. H.; Nenes, A.; Kulmala, M.; Laaksonen, A.; Facchini, M. C. *Science* **2001**, *292*, 2025.
(3) Lelieveld, J.; Crutzen, P. J.; Ramanathan, V.; Andreae, M. O.; Brenninkmeijer, C. A. M.; Campos, T.; Cass, G. R.; Dickerson, R. R.; Fischer, H.; de Gouw, J. A.; Hansel, A.; Jefferson, A.; Kley, D.; de Laat, A. T. J.; Lal, S.; Lawrence, M. G.; Lobert, J. M.; Mayol-Bracero, O. L.; Mitra, A. P.; Novakov, T.; Oltmans, S. J.; Prather, K. A.; Reiner, T.; Rodhe, H.; Scheeren, H. A.; Sikka, D.; Williams, J. *Science* **2001**, *291*, 1031.
(4) Rosenfeld, D. *Science* **2000**, *287*, 1793.
(5) Breon, F.-M.; Tanre, D.; Generoso, S. *Science* **2002**, *295*, 834.
(6) Rogge, W. F.; Mazurek, M. A.; Hildemann, L. M.; Cass, G. R.; Simoneit, B. R. T. *Atmos. Environ.* **1993**, *27*, 1309.
(7) Saxena, P.; Hildemann, L. M. *J. Atmos. Chem.* **1996**, *24*, 57.
(8) Finlayson-Pitts, B. J.; Pitts, J. N., Jr. *Chemistry of the Upper and Lower Atmosphere*; Academic Press: San Diego, CA, 2000.
(9) Raes, F.; Van Dingenen, R.; Vignati, E.; Wilson, J.; Putaud, J. P.; Seinfeld, J. H.; Adams, P. *Atmos. Environ.* **2000**, *34*, 4215.
(10) Buseck, P. R.; Posfai, M. *Proc. Natl. Acad. Sci. U.S.A.* **1999**, *96*, 3372.
(11) Zappoli, S.; Andracchio, A.; Fuzzi, S.; Facchini, M. C.; Gelencser, A.; Kiss, G.; Krivacsy, Z.; Molnar, A.; Meszaros, E.; Hansson, H. C.; Rosman, K.; Zebuhr, Y. *Atmos. Environ.* **1999**, *33*, 2733.
(12) Posfai, M.; Xu, H. F.; Anderson, J. R.; Buseck, P. R. *Geophys. Res. Lett.* **1998**, *25*, 1907.
(13) Murphy, D. M.; Thomson, D. S.; Middlebrook, A. M.; Schein, M. E. *J. Geophys. Res.* **1998**, *103*, 16 485.
(14) Gill, P. S.; Graedel, T. E. *Rev. Geophys.* **1983**, *21*, 903.
(15) Facchini, M. C.; Mircea, M.; Fuzzi, S.; Charlson, R. J. *Nature* **1999**, *401*, 257.
(16) Novakov, T.; Penner, J. E. *Nature* **1993**, *365*, 823.
(17) Matsumoto, K.; Tanaka, H.; Nagao, I.; Ishizaka, Y. *Geophys. Res. Lett.* **1997**, *24*, 655.
(18) Murphy, D. M.; Thomson, D. S.; Mahoney, T. M. J. *Science* **1998**, *282*, 1664.
(19) Middlebrook, A. M.; Murphy, D. M.; Thomson, D. S. *J. Geophys. Res.* **1998**, *103*, 16 475.
(20) Turpin, B. J.; Saxena, P.; Andrews, E. *Atmos. Environ.* **2000**, *34*, 2983.
(21) Griffin, R. J.; Cocker, D. R.; Flagan, R. C.; Seinfeld, J. H. *J. Geophys. Res.* **1999**, *104*, 3555.
(22) Hoffmann, T.; Odum, J. R.; Bowman, F.; Collins, D.; Klockow, D.; Flagan, R. C.; Seinfeld, J. H. *J. Atmos. Chem.* **1997**, *26*, 189.
(23) Tobias, H. J.; Docherty, K. S.; Beving, D. E.; Ziemann, P. J. *Environ. Sci. Technol.* **2000**, *34*, 2116.
(24) Jacobson, M. C.; Hansson, H. C.; Noone, K. J.; Charlson, R. J. *Rev. Geophys.* **2000**, *38*, 267.
(25) Cruz, C. N.; Pandis, S. N. *J. Geophys. Res.* **1998**, *103*, 13 111.
(26) Hemming, B. L.; Seinfeld, J. H. *Indust. Eng. Chem.* **2001**, *40*, 4162.
(27) Moise, T.; Rudich, Y. *Geophys. Res. Lett.* **2001**, *28*, 4083.
(28) Bertram, A. K.; Ivanov, A. V.; Hunter, M.; Molina, L. T.; Molina, M. J. *J. Phys. Chem. A* **2001**, *105*, 9415.
(29) Kotzick, R.; Panne, U.; Niessner, R. *J. Aerosol Sci.* **1997**, *28*, 725.
(30) Moise, T.; Talukdar, R. K.; Frost, G. J.; Fox, R. W.; Rudich, Y. *J. Geophys. Res.* **2001**, *107*, 10.1029/2001JD000334.
(31) Moise, T.; Rudich, Y. *J. Geophys. Res.* **2000**, *105*, 14 667.
(32) Wadia, Y.; Tobias, D. J.; Stafford, R.; Finlayson-Pitts, B. J. *Langmuir* **2000**, *16*, 9321.
(33) Poschl, U.; Letzel, T.; Schauer, C.; Niessner, R. *J. Phys. Chem. A* **2001**, *105*, 4029.
(34) de Gouw, J. A.; Lovejoy, E. R. *Geophys. Res. Lett.* **1998**, *25*, 931.
(35) Noble, C. A.; Prather, K. A. *Environ. Sci. Technol.* **1996**, *30*, 2667.
(36) Jayne, J. T.; Leard, D. C.; Zhang, X. F.; Davidovits, P.; Smith, K. A.; Kolb, C. E.; Worsnop, D. R. *Aeros. Sci. Technol.* **2000**, *33*, 49.
(37) Morris, J. W.; Davidovits, P.; Jayne, J. T.; Jimenez, J. L.; Shi, Q.; Kolb, C. E.; Worsnop, D. R.; Barney, W. S.; Cass, G. *Geophys. Res. Lett.* **2002**, *29*, 10.1029/2002GL014692.
(38) Cabalo, J.; Zelenyuk, A.; Baer, T.; Miller, R. E. *Aeros. Sci. Technol.* **2000**, *33*, 3.
(39) Smith, G. D.; Woods, I. E.; DeForest, C. L.; Baer, T.; Miller, R. E., submitted to *J. Phys. Chem. A* **2002**.
(40) Schauer, J. J.; Rogge, W. F.; Hildemann, L. M.; Mazurek, M. A.; Cass, G. R. *Atmos. Environ.* **1996**, *30*, 3837.
(41) Barger, W. R.; Garrett, W. D. *J. Geophys. Res.* **1970**, *75*, 4561.
(42) Marty, J. C.; Saliot, A.; Buat-Menard, P.; Chesselet, R.; Hunter, K. A. *J. Geophys. Res.* **1979**, *84*, 5707.
(43) Blanchard, D. C. *Science* **1964**, *146*, 396.
(44) Bezdek, H. F.; Carlucci, A. F. *Limnol. Oceanogr.* **1974**, *19*, 126.
(45) Ellison, G. B.; Tuck, A. F.; Vaida, V. *J. Geophys. Res.* **1999**, *104*, 11 633.
(46) Kawamura, K.; Semere, R.; Imai, Y.; Fujii, Y.; Hayashi, M. *J. Geophys. Res.* **1996**, *101*, 18 721.
(47) Kawamura, K.; Kaplan, I. R. *Anal. Chem.* **1984**, *56*, 1616.
(48) Donaldson, D. J.; Anderson, D. *J. Phys. Chem. A* **1999**, *103*, 871.
(49) Limbeck, A.; Puxbaum, H. *Atmos. Environ.* **1999**, *33*, 1847.
(50) Rogge, W. F.; Hildemann, L. M.; Mazurek, M. A.; Cass, G. R.; Simoneit, B. R. T. *Environ. Sci. Technol.* **1993**, *27*, 2700.
(51) Lovejoy, E. R.; Huey, L. G.; Hanson, D. R. *J. Geophys. Res.* **1995**, *100*, 18 775.
(52) Hanson, D. R.; Burkholder, J. B.; Howard, C. J.; Ravishankara, A. R. *J. Phys. Chem.* **1992**, *96*, 4979.
(53) Brown, R. L. *J. Res. Natl. Bur. Stand. U. S.* **1978**, *83*, 1.
(54) Fuller, E. N.; Schettler, P. D.; Giddings, J. C. *Indust. Eng. Chem.* **1966**, *58*, 19.
(55) Thomas, E. R.; Frost, G. J.; Rudich, Y. *J. Geophys. Res.* **2001**, *106*, 3045.
(56) Hanson, D. R.; Ravishankara, A. R. *J. Phys. Chem.* **1993**, *97*, 12 309.
(57) Kolb, C. E.; Worsnop, D. R.; Zahniser, M. S.; Davidovits, P.; Keyser, L. F.; Leu, M.-T.; Molina, M. J.; Hanson, D. R.; Ravishankara, A. R. Laboratory Studies of Atmospheric Heterogeneous Chemistry. In *Progress and Problems in Atmospheric Chemistry*; Barker, J. R., Ed.; World Scientific: 1995; Vol. 3.
(58) Danckwerts, P. V. *Trans. Faraday Soc.* **1951**, *47*, 1014.
(59) Razumovskii, S. D.; Zaikov, G. E. *Ozone and its Reactions with Organic Compounds*; Elsevier Science Publishers: 1984; Vol. 15.
(60) Grosjean, E.; Grosjean, D. *Int. J. Chem. Kinet.* **1996**, *28*, 911.
(61) Grosjean, E.; Grosjean, D. *Int. J. Chem. Kinet.* **1995**, *27*, 1045.
(62) Makar, P. A. *Atmos. Environ.* **2001**, *35*, 961.
(63) Criegee, R. *Angew. Chem., Int. Edit.* **1975**, *14*, 745.
(64) Bailey, P. S. *Ozonation in Organic Chemistry*; Academic Press: New York, 1978; Vol. 1 and 2.
(65) Morrison, R. T.; Boyd, R. N. *Organic Chemistry*; Prentice Hall: 1992.
(66) Tobias, H. J.; Ziemann, P. J. *Environ. Sci. Technol.* **2000**, *34*, 2105.
(67) Hanson, D. R.; Ravishankara, A. R.; Solomon, S. *J. Geophys. Res.* **1994**, *99*, 3615.
(68) Kawamura, K.; Steinberg, S.; Kaplan, I. R. *Atmos. Environ.* **1996**, *30*, 1035.
(69) Kawamura, K.; Yokoyama, K.; Fujii, Y.; Watanabe, O. *Geophys. Res. Lett.* **1999**, *26*, 871.
(70) Saxena, P.; Hildemann, L. M.; McMurry, P. H.; Seinfeld, J. H. *J. Geophys. Res.* **1995**, *100*, 18 755.
(71) Novakov, T.; Corrigan, C. E. *Geophys. Res. Lett.* **1996**, *23*, 2141.
(72) Blando, J. D.; Porcja, R. J.; Li, T. H.; Bowman, D.; Lioy, P. J.; Turpin, B. J. *Environ. Sci. Technol.* **1998**, *32*, 604.
(73) Mazurek, M.; Masonjones, M. C.; Masonjones, H. D.; Salmon, L. G.; Cass, G. R.; Hallock, K. A.; Leach, M. *J. Geophys. Res.* **1997**, *102*, 3779.
(74) Shulman, M. L.; Jacobson, M. C.; Carlson, R. J.; Synovec, R. E.; Young, T. E. *Geophys. Res. Lett.* **1996**, *23*, 277.